Observational insights into isoprene secondary organic aerosol formation through the epoxides pathway at three urban sites from northern to southern China

Yu-Qing Zhang[1,,2], Xiang Ding[1,2,4,], Quan-Fu He[1,#], Tian-Xue Wen[3], Jun-Qi Wang[1,6], Kong Yang[1,6], Hao Jiang[1,6], Qian Cheng[1,6], Ping Liu[1,6], Zi-Rui Wang[1,6], Yun-Feng He[1,6], Wei-Wei Hu[1,2,4], Qiao-Yun Wang[5], Jin-Yuan Xin[3], Yue-Si Wang[3], Xin-Ming Wang[1,2,4]*

[1] State Key Laboratory of Organic Geochemistry and Guangdong Provincial Key Laboratory of Environmental Protection and Resources Utilization, Guangzhou Institute of Geochemistry, Chinese Academy of Sciences, Guangzhou 510640, China
[2] CAS Center for Excellence in Deep Earth Science, Guangzhou 510640, China
[3] Institute of Atmospheric Physics, Chinese Academy of Sciences, Beijing 100029, China
[4] Guangdong-Hong Kong-Macao Joint Laboratory for Environmental Pollution and Control, Guangzhou Institute of Geochemistry, Chinese Academy of Science, Guangzhou 510640, China
[5] School of Chemical Engineering and Technology, Guangdong Industry Polytechnic, Guangzhou 510300, China
[6] University of Chinese Academy of Sciences, Beijing 100049, China

TOC

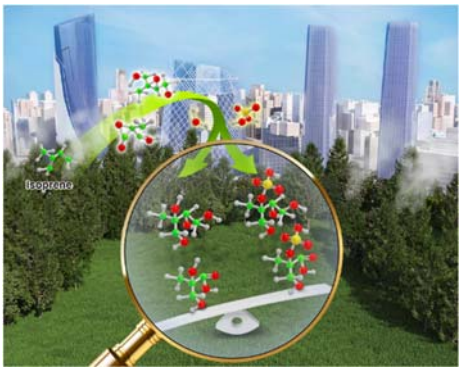

SYNOPSIS: Isoprene epoxides are more likely to react with water than sulfate through IEPOX-pathway in urban air.

KEYWORDS: isoprene epoxides, secondary organic aerosols, formation mechanism, nucleophilic addition reaction, aqueous reaction

ABSTRACT

Isoprene is the most abundant precursor of global secondary organic aerosol (SOA). The epoxides pathway plays a critical role in isoprene SOA (iSOA) formation, in which isoprene epoxydiols (IEPOX) and/or hydroxymethyl-methyl-α-lactone (HMML) can react with nucleophilic sulfate and water producing isoprene-derived organosulfates (iOSs) and oxygen-containing tracers (iOTs), respectively. This process is complicated and highly influenced by anthropogenic emissions, especially in the polluted urban atmospheres. In this study, we took a one-year measurement of the paired iOSs and iOTs formed through the IEPOX and HMML pathways at the three urban sites from northern to southern China. The annual average concentrations of iSOA products at the three sites ranged from 14.6 to 36.5 ng m^{-3}. We found that the nucleophilic-addition reaction of isoprene epoxides with water dominated over that with sulfate in the polluted urban air. And a simple set of reaction rate constant could not fully describe iOSs and iOTs formation everywhere. We also found that the IEPOX-pathway was dominant over the HMML-pathway over urban regions. And using the kinetic data of IEPOX to estimate the reaction parameters of HMML will cause significant underestimation in the importance of HMML pathway. All these findings provide insights into iSOA formation over polluted areas.

1. INTRODUCTION

Isoprene (2-methyl-1,3-butadiene, C_5H_8) is the largest single hydrocarbon released into the atmosphere from vegetation. Due to its high reactivity, isoprene can be rapidly oxidized in the atmosphere to form secondary organic aerosol (SOA). As compared with other SOA precursors, isoprene alone accounts for about half of the annual global emissions (about 400-500 TgC yr^{-1})[1-3] and could contribute up to ~70% of the total SOA.[4-6] Moreover, the production of isoprene SOA (iSOA) could be highly influenced by anthropogenic emissions (such as SO_x, NO_x and OA), especially in the polluted urban atmospheres.[7-9] Both field and laboratory studies have demonstrated that the increases in SO_2 and sulfate greatly stimulate iSOA formation.[10, 11] NO_x is generally associated with reduced SOA yield from isoprene.[12, 13] The yield of iSOA could increase with high OA mass loadings in a pollution plume.[8] Considering the significant impact of iSOA on air quality and climate change,[11, 14] observational insights are of great importance to provide comprehensive understandings of iSOA chemistry in the real atmosphere.

The epoxide pathway plays a critical role in iSOA formation. The isoprene epoxydiols (IEPOX) and hydroxymethyl-methyl-α-lactone (HMML) are key reactive intermediates in the gas phase under low-NO_x and high-NO_x conditions, respectively.[15, 16] Further particulate uptake of and nucleophilic addition toward isoprene epoxides produce iSOA.[17] In the real atmosphere, sulfate and water are both strong nucleophiles in particles.[18] And the nucleophilic addition reactions of sulfate and water toward

isoprene epoxides are competitive with each other (Figure 1a), yielding organosulfates (iOSs, such as 2-methyltetrol-OS and 2-methylglyceric acid-OS) and oxygen-containing tracers (iOTs, such as 2-methyltetrols and 2-methylglyceric acid), respectively.[19-21] In addition, the acid-catalyzed intramolecular rearrangement of IEPOX in the particle phase can also produce the low-NO_x products, e.g., 3-MeTHF-3,4-diols and C_5-alkenetriols.[22] Thus, it is essential to distinguish the relative importance of the competitive nucleophilic addition reactions of sulfate and water to isoprene epoxides.

There is a large difference in the relative abundances of iOSs and iOTs among previous field, chamber and modeling studies, although the comparison of quantitative results between different studies is associated with uncertainties due to the absence of authentic standards. Table S1 lists the data of paired iOTs and iOSs that both reported in a study. In the ambient air, 2-methyltetrols (2-MTO, 0.14-573 ng m^{-3}) were always dominant over 2-methyltetrol-OS (2-MTOOS, undetectable-207 ng m^{-3}),[9, 21-26] while in the chamber and modeling studies, the relative abundances of 2-MTO and 2-MTOOS varied under different simulation conditions.[26-31] For the HMML-derived iSOA products, 2-methylglyceric acid (2-MGA) was dominant over 2-methylglyceric acid-OS (2-MGAOS) in the chamber and modeling studies,[26-31] while the relative abundances of 2-MGA (0.86-25.9 ng m^{-3}) and 2-MGAOS (undetectable-13.6 ng m^{-3}) varied in the atmospheres of different places.[9, 21-26]

The discrepancy between modeling and field studies should be largely due to the

uncertainty in aqueous kinetic parameters and Henry's law constants used in models. As summarized by Brüggemann et al.,[32] the kinetic rates of IEPOX reacting with water and sulfate varied by one and three orders of magnitude, respectively, and the Henry's law constants of IEPOX differed by two orders of magnitude in different studies. Moreover, the presence of NO_x enables iSOA formation through the HMML pathway.[16, 20] The coexistence of the competitive IEPOX and HMML reactions in the ambient air indeed leads to large changes in chemical composition of iOSs and iOTs.[19] At present, there are limited experimental data for the multiphase reactions of HMML,[16] and most parameters for HMML related reactions in model are assumed to be the same as those for IEPOX.[27] Thus, it is necessary to carry out large scale concurrent observation of both iOSs and iOTs to constrain their distribution in model results.

In this study, a one-year measurement was undertaken simultaneously at three urban sites from northern to southern China, covering different temperate zones, vegetation types and pollution conditions (Table S2). For the first time, we measured the paired iOSs and iOTs formed through the IEPOX- and HMML-pathways on a large national scale to study the spatial and seasonal characteristics of iSOA. Moreover, based on the iSOA composition and kinetic calculation, we provided insight into the relative importance of two major competitive reactions in iSOA formation: 1) competitive reactions of isoprene epoxides with water and sulfate, 2) competitive reactions of IEPOX- and HMML-pathways. These results enrich our knowledge and scientific understanding in iSOA chemistry over polluted regions.

2. EXPERIMENTAL SECTION

2.1. Field Sampling. Sampling was performed simultaneously from November 2013 to November 2014 in three cities of China. Beijing (BJ) is located in the Beijing-Tianjin-Hebei (BTH) region of northern China where vegetation is dominated by broadleaf deciduous trees. Hefei (HF) is situated in the Yangtze River Delta (YRD) region of eastern China where coniferous and broadleaf deciduous trees are major vegetation. Kunming (KM) lies in the southwestern China where has large-scale land coverage of broadleaf evergreen trees as well as high temperature and strong solar radiation all year round. BTH and YRD are two of the most developed regions in China. KM is the third largest city in the southwestern China. Thus, the three cities cover different vegetation and pollution scenarios from northern to southern China. Detail information of the cities and sampling sites were shown in Table S2 and Text S1.

Size-segregated particle samples were collected on prebaked quartz fiber filters (Whatman, 500 °C for 10 h) using the Anderson samplers equipped with nine-stage cascade impactors. The airflow rate of each sampler was 28.3 L min^{-1} and was calibrated before and after sampling. One set of nine size-fractionated filters was collected 48 hours biweekly and stored at -20 °C after sampling. A total of 76 sets of field samples were collected along with a set of field blanks at each site. This study was a sub-project of the Campaign on Atmospheric Aerosol Research network of China (CARE-China) which primarily aimed at size distribution of particulate matter and its major components over China.[33] For one set of 9 filters, each was divided into two parts. One

was used for iSOA products analysis in our laboratory. The other was sent to other groups for measuring major components to determine their size distribution.

2.2. Chemical Analysis. Considering the analytical limitation, we combined each set of nine filters as one sample. We added the standard mixtures of $^{13}C_6$-levoglucosan and ketopinic acid as internal standards. After that, each sample was extracted three times by sonication with 60 mL methanol each time. The extracts were combined into a solution which was further concentrated, centrifuged, syringe filtered and finally divided into two aliquots. One was blown to dryness under gentle nitrogen and was redissolved in 200 μL of a 1:1 (v:v) solvent mixture of 0.1% acetic acid in water and 0.1% acetic acid in methanol.[34] The other was blown to dryness under gentle nitrogen and was redissolved in 50 μL of pyridine, then silylated with 100 μL of N,O-bis-(trimethylsilyl)-trifluoroacetamide plus 1% trimethylchlorosilane at 70 °C for one hour.[35]

The aliquot redissolved in water and methanol was analyzed for iOSs by an Agilent 6410 Triple Quadrupole liquid chromatography (LC) tandem mass spectrometer (MS) equipped with an electrospray ionization (ESI) source in the negative ion mode. The instrument was operated in the full scan mode using a Waters Atlantic T3 column (3 μm; 2.1 × 250 mm). The pressure of the ESI nebulizer was 0.8 bar and the dry gas flow was 10 L min^{-1}, ionization voltage and the fragmentor was 4 kV and 120 V respectively. The eluents consisted of water with 0.1% acetic acid (eluent A) and methanol (eluent B) with a total flow rate of 0.2 mL min^{-1}. The mobile-phase gradient was set as 3% B

149 at the beginning and held for 5 min, B increased to 90% in 25 min and held for 10 min,
150 then B increased to 95% in 2 min and held for 6 min, finally B decreased to 3% in 5
151 min and held for 12 min. iOSs were quantified using camphor sulfonic acid as the
152 surrogate.

153 The silylated aliquot was analyzed for iOTs, C_5-alkenetriols, and 3-MeTHF-3,4-
154 diols by an Agilent 7890/5975C gas chromatography (GC)/mass spectrometer detector
155 (MSD) using a 30 m HP-5 MS capillary column (i.d., 0.25 mm; film thickness, 0.25
156 μm) with an electron impact (EI) ionization source in the selected ion monitoring (SIM)
157 mode. The GC temperature was initiated at 65 °C and held for 2 min, then increased to
158 290 °C at the rate of 5 °C min^{-1} and held for 20 min. The iOTs, C_5-alkenetriols, and 3-
159 MeTHF-3,4-diols were quantified using erythritol as the surrogate. The detailed
160 information about the parameters and data extraction of LC-MS and GC-MS were
161 described elsewhere.[34, 35]

162 The data of daily maximum solar radiation (W m^{-2}), mean temperature (°C) and
163 relative humidity (RH, %) during each sampling episode in the three cities were
164 downloaded from the China Meteorological Data Sharing Service System
165 (http://data.cma.cn/).

166 **2.3. Estimation of reaction rates for isoprene epoxides**

167 The rate determining step of the acid-catalyzed ring-opening reaction of an
168 epoxide is a concerted nucleophilic addition to the ring.[18] The pseudo-first-order rate
169 constants (k_{aq}) for an epoxide to particle phase could be estimated as equation (1).[18]

$$k_{aq} = \sum_{i=1}^{N} \sum_{j=1}^{M} k_{i,j} [nuc_i]_{aq} [acid_j]_{aq} \quad (1)$$

Where N and M represent the number of nucleophiles and acids, respectively, $k_{i,j}$ are the third-order rate constants of isoprene epoxides with nucleophile *i* and acid *j* in aqueous-phase reactions ($k_{i,j}$ values from literatures were shown in Table S3),[27, 28, 36] $[nuc_i]_{aq}$ and $[acid_j]_{aq}$ represent the molarity (mol L^{-1}) of nucleophile *i* (water and sulfate) and acid *j* (H^+ and HSO_4^-), respectively. The reaction rate constant of isoprene epoxides reacting with water (k_{aq_water}) could be calculated as $k_{water,H+}[H_2O][H^+] + k_{water,HSO4-}[H_2O][HSO_4^-]$, and the reaction rate constant of isoprene epoxides reacting with sulfate ($k_{aq\_sulfate}$) could be calculated as $k_{SO42-,H+}[SO_4^{2-}][H^+] + k_{SO42-,HSO4-}[SO_4^{2-}][HSO_4^-]$. Detail information about the estimation of aerosol acidity and water content as well as the influence of organic acid on aerosol acidity could be found in Text S2.

The uptake coefficient (γ) of an epoxide can be estimated using equation (2)-(4):[10, 27]

$$\frac{1}{\gamma} = \frac{1}{\alpha} + \frac{\omega}{4H_{epoxide}RT\sqrt{D_a k_{aq}}} \frac{1}{f(q)} \quad (2)$$

$$f(q) = \coth(q) - \frac{1}{q} \quad (3)$$

$$q = r_p \sqrt{\frac{k_{aq}}{D_a}} \quad (4)$$

where α is the mass accommodation coefficient of an epoxide (0.1 for IEPOX),[37, 38] ω is the mean molecular speed of an epoxide (e.g., 231 m s^{-1} for IEPOX at 298K),[10] Da is the diffusivity of an epoxide in the aqueous phase (e.g., 10^{-9} m^2 s^{-1} for IEPOX),[27] R is the gas constant (L atm mol^{-1} K^{-1}), T is temperature (K), r_p is the effective radius (m) which could be calculated from wet particle diameter (Text S3), $H_{epoxide}$ is the Henry's

Law coefficient of an epoxide (1.3×10^8 M atm^{-1} for IEPOX and 7.5×10^6 M atm^{-1} for HMML),[18, 39] and k_{aq} for an epoxide could be calculated using equation (1).

The pseudo-first-order heterogeneous reaction rate constant (k_{het}, s^{-1}) of an epoxide on particles describes the overall reaction rate of epoxide uptake to particles and subsequent aqueous-phase reactions. Considering the negligible impact of the gas phase diffusion on this process,[37] k_{het} can be estimated using equation (5):[10]

$$k_{het} = \frac{\gamma \omega S_a}{4} \quad (5)$$

where γ is the uptake coefficient of an epoxide, ω value is the same as that used in equation (2), S_a is the surface area of particles at ambient RH, which could be estimated based on size distribution of dry particles and their hygroscopic growth factors in the κ-Köhler theory (Text S3).[10, 40]

2.4. Quality Assurance/Quality Control (QA/QC).

Field and laboratory blank samples were analyzed together with these ambient samples. The target iSOA products were not detected in these blank samples. Relative differences for target compounds in paired duplicate samples (n = 7) were all < 5%. As the lack of authentic standards, camphor sulfonic acid and erythritol were used to determine the recoveries and detection limits of the iSOA products. Recoveries of camphor sulfonic acid and erythritol in seven spiked samples were 95 ± 5% and 85 ± 4%, respectively. The detection limits for camphor sulfonic acid and erythritol were 0.01 ng m^{-3} and 0.04 ng m^{-3}, respectively, which were determined by seven successive injections of standard solutions. The errors of sample analysis (E_A) that included

surrogate quantification, field blank, analytical repeatability and recovery were estimated to be 22%, 26%, 38%, 86%, 215%, and 230% for 2-MTO, 2-MGA, 3-MeTHF-3,4-diols, C_5-alkenetriols, 2-MTOOS, and 2-MGAOS, respectively using the method suggested by Stone et al. (2012)[41] (Text S4 and Table S9).

Sulfate might have co-eluted with iOSs and changed the ESI conditions during LC-MS analysis. In our previous study, we analyzed 2-MTOOS and 2-MGAOS in parallel filters with different sulfate concentrations. Our results demonstrated that the impact of sulfate on iOSs quantification could be ignored.[21] The measured iOTs might partly come from thermal decomposition of iOSs during the GC-MS analysis.[26] In this study, average concentration of iOSs (2.26 ng m^{-3}) was much lower than that of iOTs (20.2 ng m^{-3}) by a factor of ~9. Thus, even if all iOSs converted into iOTs during the silylation and GC-MS analysis processes, the thermal degradation of iOSs would only generate 7% of GC-MS measured iOTs. Thus, the overall uncertainty for iOTs analysis that estimated through the error propagation of E_A and thermal degradation was 16%.

3. RESULTS AND DISCUSSION

3.1. Average Composition

As Figure 1b presented, 2-MTO was the predominant species, accounting for 50% (7.52-25.1 ng m^{-3}) of all iSOA products at three sites, followed by 2-MGA (18%, 2.76-4.37 ng m^{-3}), C_5-alkenetriols (17%, 2.68-5.04 ng m^{-3}), 2-MGAOS (9%, 0.99-1.68 ng m^{-3}), 2-MTOOS (6%, 0.50-1.43 ng m^{-3}), and 3-MeTHF-3,4-diols (1%, 0.14-0.32 ng m^{-3}). Annual averages of iOSs (2-MTOOS and 2-MGAOS) were 1.49 ± 1.17 ng m^{-3}, 2.38 ±

2.51 ng m^{-3} and 2.92 ± 1.42 ng m^{-3} in BJ, HF and KM, respectively (Figure S2). Annual average of the paired iOTs (2-MTO and 2-MGA) were 10.3 ± 15.0 ng m^{-3}, 22.0 ± 28.2 ng m^{-3} and 28.3 ± 18.9 ng m^{-3} in BJ, HF and KM, respectively (Figure S2). The levels of iOTs were higher than those of iOSs by factors of 5.8-11. Table S10 shows the carbon fractions of these iSOA products in OC at the three sites. Annual averages of iSOA products/OC ranged from 0.24-0.80 ‰. KM had the highest OC fractions of iOTs (0.63 ± 0.55 ‰), iOSs (0.04 ± 0.02 ‰), and C_5-alkenetriols (0.13 ± 0.11 ‰), followed by HF and BJ. Since 3-MeTHF-3,4-diols were in the trace amount, their OC fractions were 1-2 orders of magnitude lower than other iSOA products.

The iSOA products formed through the IEPOX pathway (IEPOX-SOA products) were composed of 2-MTOOS, 2-MTO, C_5-alkenetriols and 3-MeTHF-3,4-diols. Annual averages of the IEPOX-SOA products were 10.8 ± 16.6 ng m^{-3} in BJ, 23.5 ± 32.1 ng m^{-3} in HF and 31.7 ± 21.2 ng m^{-3} in KM (Figure S2). 2-MGAOS and 2-MGA are typical iSOA products formed through the HMML pathway (HMML-SOA products). Annual averages of HMML-SOA products were 3.75 ± 4.03 ng m^{-3}, 6.04 ± 5.46 ng m^{-3} and 4.75 ± 2.13 ng m^{-3} in BJ, HF and KM, respectively (Figure S2). Compared with the IEPOX-SOA products, the HMML-SOA products were lower by factors of 2.1-6.4, probably due to lower yields of iSOA through the high NO_x pathway.[13] Annual average OC contributions of IEPOX- and HMML-SOA products ranged from 0.19 - 0.72 ‰ and 0.05 - 0.09 ‰, respectively among the three sites. The highest OC fraction of IEPOX- SOA products occurred at the KM site while that of HMML- SOA products existed at the HF site (Table S10). Since these SOA products

were all originated from isoprene, they correlated well with each other ($p < 0.01$, Table S11). Table S12 lists the concentrations of all iSOA products at the three sites.

3.2. Spatial and seasonal variations of iSOA products

Figure 1b presents spatial distribution of iSOA products. KM had the highest levels (36.5 ± 22.8 ng m^{-3}), followed by HF (29.6 ± 37.4 ng m^{-3}) and BJ (14.6 ± 20.4 ng m^{-3}). Such a spatial difference of annual average of iSOA products should be determined by the spatial and seasonal variations of isoprene emission in China. Isoprene is mainly emitted from broadleaf trees and its emission rate is affected by temperature and solar radiation.[42] As compared with KM, BJ and HF sites had higher temperature during summer but lower temperature and solar radiation in other seasons (Table S12). Therefore, it is expected that BJ and HF have higher isoprene emission in summertime, while KM has stronger isoprene emission in other seasons. In fact, the concentrations of iSOA products in both BJ and HF were higher than KM during the summer but lower in other seasons (Figure S3). Thus, the relatively low levels of annual average iSOA products in BJ and HF were mainly ascribed to relatively low isoprene emission due to the relatively low temperature and sunlight intensity during the seasons other than summer.

Figure 2 exhibits monthly variations of different iSOA products at the three sites. Higher concentrations of total iSOA products were observed in the summer (on average 40.5 ng m^{-3} in BJ and 69.1 ng m^{-3} in HF) and fall (on average 52.1 ng m^{-3} in KM), and lower levels were found in the winter (on average 3.59 ng m^{-3}, 5.98 ng m^{-3} and 23.6 ng

m^{-3} in BJ, HF and KM, respectively). The highest levels of iOTs, iOSs (Figure 2 a-c), IEPOX- and HMML-SOA products (Figure 2 d-f) occurred in August, July and October in BJ, HF and KM, respectively. High temperature and strong solar radiation in the warm period could promote isoprene emission and favor isoprene oxidation in the air. The leaf senescence and low temperature during winter could reduce isoprene emission sharply in the cold period. Thus, it is expected that the seasonal changes of iSOA levels in BJ and HF were highly related to the variations of solar radiation and temperature there. The KM site was located in the sub-humid warm temperate zone where was characterized as large-scale land cover of broadleaf evergreen trees and narrow ranges of change in temperature (15.9 ± 5.00 ºC) and solar radiation (947 ± 233 W m^{-2}) during our sampling. Thus, the seasonal variation of iSOA in KM might not fully follow the changes of solar radiation and temperature there. Besides solar radiation and temperature, other factors including leaf age, soil moisture, leaf area index and CO_2 concentrations also affect isoprene emission.[42]

3.3 Competitive reactions of isoprene epoxides with water and sulfate

As suggested by Eddingsaas et al. (2010), the acid-catalyzed ring-opening reaction of an epoxide was via protonation of the epoxide oxygen and nucleophilic addition.[18] Thus, the iOSs and iOTs could be produced from the nucleophilic-addition reactions of isoprene epoxides (IEPOX and HMML) with sulfate and water, respectively, on acidic particles (Figure 1a). As Figure S4 showed, both iOSs and iOTs negatively correlated with aerosol pH ($p<0.05$), indicating that stronger atmospheric acidity could stimulate

297 the formation of iOSs and iOTs. Although sulfate and water are major nucleophiles in
298 particles, the poor correlations of iOSs with sulfate and iOTs with water implied that
299 the formation of iOSs and iOTs would not be controlled by nucleophiles alone.

300 In the ambient air, the reactions of isoprene epoxides with sulfate and water coexist
301 and are competitive with each other. The relative abundance of iOSs and iOTs can be
302 used to diagnose the relative importance of sulfate- and water-addition reactions with
303 isoprene epoxides. The annual averages of iOSs to iOTs ratio (iOSs/iOTs) were 0.53 in
304 BJ, 0.25 in HF, and 0.12 in KM (Figure S5 and Table S12). This indicated that the
305 nucleophilic-addition reaction of water to isoprene epoxides was generally more
306 effective than that of sulfate. In summer the iOSs/iOTs ratios at the three sites were
307 close, while in other seasons, BJ had the highest ratio of iOSs/iOTs, followed by HF
308 and KM (Figure S5). This suggested that the nucleophilic-addition reaction of isoprene
309 epoxides with sulfate in BJ played more important role in iSOA formation as compared
310 with that in HF and KM. The ratios of iOSs/iOTs, 2-MTOOS/2-MTO and 2-MGAOS/2-
311 MGA all increased in fall and winter, and decreased in the summer (Figure 2 a-c and
312 Figure S6), suggesting the increasing importance of sulfate-addition reaction in cold
313 period. This was more apparent at the BJ site that the ratios of iOSs/iOTs, 2-MTOOS/2-
314 MTO and 2-MGAOS/2-MGA exceeded 1.0 in the fall and winter samples (Figure 2 a
315 and Figure S6 a, d). Thus, the nucleophilic-addition reaction of isoprene epoxides with
316 sulfate was dominant over that of water during cold period in BJ.

317 We further calculated the k_{aq} values for isoprene epoxides with water and sulfate,

318 respectively using equation (1).[18] Obviously, the $k_{i,j}$ values are critical in the k_{aq}
319 calculation (especially k_{i,H^+}). Pye et al. (2013) and Riedel et al. (2016) estimated the $k_{i,j}$
320 values using models with the constraint of ambient measurements and chamber
321 experiments, respectively. Piletic et al. (2013) estimated the $k_{i,j}$ values based on the
322 computational calculation. Table S3 lists the available $k_{i,j}$ values for isoprene
323 epoxides.[27, 28, 36] The $k_{i,j}$ values provided by Pye et al. (2013) (k_{i,H^+}-1=9.0 × 10^{-4} M^{-2} s^{-1}
324 for water, and 2.0 × 10^{-4} M^{-2} s^{-1} for sulfate) and Riedel et al. (2016) (k_{i,H^+}-2 =3.4 × 10^{-}
325 ^{4} M^{-2} s^{-1} for water, and 4.8 × 10^{-4} M^{-2} s^{-1} for sulfate) were comparable but were 2-3
326 orders of magnitude lower than those provided by Piletic et al. (2013) (k_{i,H^+}-3=5.3 ×
327 10^{-2} M^{-2} s^{-1} for water, and 5.2 × 10^{-1} M^{-2} s^{-1} for sulfate). Due to the lack of kinetic data
328 for HMML, in this study the HMML rate constants were assumed to be the same as
329 those for IEPOX.[27]

330 Figure 3 presents the $k_{aq\_sulfate}$ /k_{aq_water} ratios calculated using the $k_{i,j}$ values
331 reported in different studies. The ratios of paired iSOA products (iOSs/iOTs, 2-
332 MGAOS/2-MGA and 2-MTOOS/2-MTO) all positively correlated with the ratios of
333 $k_{aq\_sulfate}$ /k_{aq_water} ($p < 0.05$, Table S13), demonstrating that the seasonal variations of
334 iOSs/iOTs ratios were determined by the relative importance of aqueous phase reaction
335 rates of isoprene epoxides with sulfate and water. Using the $k_{i,j}$ values suggested by Pye
336 et al. (2013) (k_{i,H^+}-1)[27] and Riedel et al. (2016) (k_{i,H^+}-2),[28] the $k_{aq\_sulfate}$/k_{aq_water} ratios at
337 the three sites were all lower than one. This was consistent with our observation of
338 iOSs/iOTs ratios at the three sites, except iOSs/iOTs ratios higher than one in fall and
339 winter at the BJ site (Figure 2a). All these results demonstrated that the nucleophilic

addition of water to isoprene epoxides was more effective than that of sulfate in the urban atmosphere.

It must be pointed out that the gradient order of the $k_{aq\_sulfate}/k_{aq\_water}$ ratio was BJ > KM > HF using a single set of $k_{i,j}$ values. In fact, however, the observed order of iOSs/iOTs ratio was BJ > HF > KM (Figure 3). Moreover, we did see elevated iOSs/iOTs ratios beyond one, even as high as 2.90 during the winter at the BJ site (Figure 2a). Using the k_{i,H^+}-1 and k_{i,H^+}-2 values we could not repeat such high ratios of $k_{aq\_sulfate}/k_{aq\_water}$. Applying the k_{i,H^+}-3 values suggested by Piletic et al. (2013)[36] could increase the $k_{aq\_sulfate}/k_{aq\_water}$ ratio reaching 8.01. However, it led to the $k_{aq\_sulfate}/k_{aq\_water}$ ratios at the three sites all beyond one (Figure 3), which was apparently inconsistent with our observation of the iOSs/iOTs ratios at the three sites. Thus, $k_{i,j}$ values might be varied under different conditions, and a simple set of $k_{i,j}$ values could not fully describe the atmospheric processes of iOSs and iOTs formation everywhere. Local parameters, such as the $k_{i,j}$ values are necessary to estimate iSOA production when models simulate iSOA distribution over a broad area.

3.4 Competitive reactions of HMML- and IEPOX-pathways

The formation of iSOA is profoundly affected by NO_x levels. As Figure 1a showed, iSOA is formed mainly through the IEPOX-pathway in the pristine atmosphere (Low-NO_x or NO_x free conditions), while the HMML-pathway plays a critical role in the polluted atmosphere (High-NO_x conditions).[19, 20] The relative abundances of HMML- and IEPOX-SOA products can be used to diagnose the impact of NO_x on iSOA

formation.[43] For instance, in the chamber studies, the elevated ratios of NO_x to isoprene led to apparent increase in the ratios of 2-MGA to 2-MTO.[44-46]

In this study, the annual average ratios of HMML-SOA products to IEPOX-SOA products were 0.60, 0.44 and 0.18 in BJ, HF and KM, respectively (Table S12). The dominance of IEPOX-SOA products over HMML-SOA products was similar to our observation during the highly polluted period over the Pearl River Delta (PRD) region, South China.[21] Based on the kinetic calculation, especially using the widely used Kintecus model,[18, 39, 47] we found that low aerosol pH and high temperature in the PRD could promote heterogeneous reactions of IEPOX and suppress the production of HMML, respectively. Thus, the IEPOX-pathway could dominate over the HMML-pathway in the iSOA formation even in the air of highly polluted areas.[21] Moreover, the ratios of HMML-/IEPOX-SOA products at the three sites all increased in fall and winter, and decreased in the summer (Figure 2d-f), suggesting the increasing importance of HMML-SOA formation pathway in the cold period.

In this study, we estimated the uptake coefficient (γ) and pseudo-first-order heterogeneous reaction rate constant (k_{het}, s^{-1}) for IEPOX (γ_{IEPOX} and k_{het_IEPOX}) and HMML (γ_{HMML} and k_{het_HMML}) using the different $k_{i,j}$ values (Table S14).[27, 28, 36] Due to the lack of kinetic data, the values used for HMML in this study were assumed to be the same as those for IEPOX, except the Henry's Law coefficient.[27] The estimated values of γ_{IEPOX} (5.34×10^{-6}-2.84×10^{-3}) at the three sites were one order of magnitude higher than those for γ_{HMML} (3.08×10^{-7}-2.01×10^{-4}). This indicated that the uptake coefficient

of IEPOX was much higher than that of HMML in the ambient air. Organic coating and relative humidity (RH) could affect the uptake coefficient of epoxides. A recent study found that phase separation can occur at RH values lower than 50% in organic aerosols.[48] The γ_{IEPOX} could decline by 30-50% in the presence of α-pinene SOA coating on the acidic sulfate particles.[49] However, the increase in RHs (e.g., > 50%) could compromise the impact of SOA coating on γ_{IEPOX}.[49] In this study, the average values of RH were 49%, 73%, and 68% in BJ, HF and KM, respectively. Therefore, the influence of OA coating might have limited influence on γ_{IEPOX} under the high RH conditions.

The estimated k_{het_IEPOX} values at the three sites using different $k_{i,j}$ were in the range of 2.42×10^{-7} s^{-1}-1.03×10^{-4} s^{-1} (Table S14). As compared with the k_{het_IEPOX} reported in Nanjing (7.12×10^{-8} s^{-1}),[50] the estimated k_{het_IEPOX} values at the three sites were higher by factors of 3-5 using the $k_{i,j}$ provided by Riedel et al. (2016).[28] The estimated values of k_{het_HMML} at the three sites were in the range of 1.40×10^{-8} s^{-1}-7.04×10^{-6} s^{-1} (Table S14). The values of k_{het_IEPOX} at the three sites were higher than those of k_{het_HMML} by a factor of 16.9-17.3, indicating that the heterogeneous reaction rate of IEPOX was much faster than that of HMML in the ambient air. In addition, as the precursor of HMML, MPAN can react with the OH radical to form HMML and decompose rapidly at high temperature (e.g., > 20 °C).[39, 51] The pathway fractions of MPAN+OH process ($k_{MPAN+OH}\% = k_{MPAN+OH} / (k_{MPAN+OH} + k_{MPAN\_decomposition})$) in BJ, HF and KM were on average 58%, 62% and 67% respectively (Text S6). This would further lower the relative importance of HMML-pathway, since not all MPAN can form HMML.

The kinetic data suggested that the HMML-pathway might have a minor contribution to iSOA formation. However, in fact, annual average ratios of HMML- to IEPOX-SOA products ranged from 0.18 to 0.60 at the three sites. The BJ site even witnessed the ratio as high as 1.21 (Table S12). Thus, the HMML-pathway should have important contributions to iSOA formation. The large discrepancy between the field observation and kinetic calculation might be mainly due to the lack of kinetic data for HMML. Currently, most kinetic parameters of HMML are assumed to be same as those of IEPOX.[27] In a modelling study, the simulated HMML-SOA product (2-MGA) over China was biased low by 67% as compared with our observation at 12 sites across China.[31] Thus, k_{het_HMML} should be underestimated by using the kinetic parameters of IEPOX.

To address the issue, we roughly estimated the kinetic data for the HMML-pathway based on the observed ratios of HMML- to IEPOX-SOA products at the three sites. Assuming that the ratio of HMML- to IEPOX-SOA products was equal to the ratio of $k^{obs}_{het\_HMML}$ to k_{het_IEPOX}, the observation-constrained heterogeneous reaction rate of HMML ($k^{obs}_{het\_HMML}$) could be estimated as:

$$k^{obs}_{het\_HMML} = k_{het\_IEPOX} \times \frac{\text{HMML-SOA products}}{\text{IEPOX-SOA products}} \quad (6)$$

The estimated $k^{obs}_{het\_HMML}$ values were in the range of 6.44×10^{-8} s^{-1}-3.73×10^{-5} s^{-1} at the three sites (Table S14). Figure 4 and Figure S7 show seasonal difference between $k^{obs}_{het\_HMML}$ and k_{het_HMML} at the three sites. Compared with k_{het_HMML}, $k^{obs}_{het\_HMML}$ increased by a factor of 9.8-10 in BJ, 7.2-7.3 in HF, and 3.0-3.1 in KM. The ratios of $k^{obs}_{het\_HMML}$ to

425 k_{het_HMML} were all highest in winter but significantly decreased in summer (BJ and HF)
426 and fall (KM). It should be noted that the k_{het_IEPOX} values were still higher than the $k^{obs}_{het\_HMML}$
427 values by factors of 2.3-6.5 at the three sites, indicating that the reactive uptake
428 of IEPOX was indeed more efficient than that of HMML in the urban air.

429 **3.5. Atmospheric Implications**

430 In this study, our results of iSOA products at three urban sites in China indicate
431 that the nucleophilic-addition reaction of isoprene epoxides with water is dominant over
432 that of sulfate in the polluted air. And a simple set of reaction rate constant could not
433 fully describe iOSs and iOTs formation everywhere. The IEPOX-pathway dominates
434 over the HMML-pathway in iSOA formation over urban regions. And based on the
435 observation, we find that the available kinetic parameters of heterogeneous reactions
436 for isoprene epoxides could not fully describe formation processes of iSOA in the real
437 atmosphere. Especially for the HMML pathway, using the kinetic data of IEPOX to
438 estimate the heterogeneous reaction parameters of HMML will cause significant
439 underestimation, which is the reason why the current models underestimate the
440 importance of HMML pathway in iSOA formation.

441 It should be noted that, although the measured iSOA products are mainly formed
442 through the IEPOX and HMML pathways on acidic particles, they could be generated
443 through other routes. Riva et al., (2016) found that 2-MTO and 2-MTOOS could be
444 produced in the isoprene ozonolysis and 1,2-ISOPOOH oxidation experiments.[52, 53]
445 Jaoui et al., (2019, 2021) proposed that the peroxy and alkoxy radical isomerization

pathways could generate highly oxygenated molecular compounds as well as 2-MTO in the gas phase.[54, 55] In addition, in the particle phase, 2-MTO could be generated though the decomposition of 2-MTO-related oligomers,[56] organosulfates[26] and organonitrates.[36] Moreover, the loss of particle-phase 2-MTO could happen due to aqueous hydroxyl radical oxidation[57]. And heterogeneous hydroxyl radical oxidation of 2-MTOOS could form more oxygenated/functionalized OSs.[58] In the ambient air, the measured iSOA products were the combined results of all these formation and loss processes. Therefore, besides the field observation, it is urgent to measure the kinetic parameters of authentic isoprene epoxides under atmospherically relevant conditions.

SUPPORTING INFORMATION

Additional description of methodology and sampling sites; additional figures and tables of iSOA products and kinetic parameters are available.

NOTES

The authors declare no competing financial interest.

ACKNOWLEDGMENTS

This research was supported by the National Key Research and Development Program (2018YFC0213902), Chinese Academy of Sciences (QYZDJ-SSW-DQC032), National Natural Science Foundation of China (42177090/41722305), Guangdong Foundation for Program of Science and Technology Research (2019B121205006/2017BT01Z134), and State Key Laboratory of Organic

Geochemistry (SKLOG2020-5).

AUTHOR INFORMATION

Corresponding Author

Xiang Ding - Guangzhou Institute of Geochemistry, Chinese Academy of Sciences (CAS), Guangzhou, 510640, China; orcid.org/0000-0002-1218-1879; Phone: 86-20-85290127; Email: xiangd@gig.ac.cn; Fax: 86-20-85290706

Authors

Yu-Qing Zhang - Guangzhou Institute of Geochemistry, CAS, Guangzhou 510640, China

Quan-Fu He – Guangzhou Institute of Geochemistry, CAS, Guangzhou 510640, China

Tian-Xue Wen - Institute of Atmospheric Physics, CAS, Beijing 100029, China

Jun-Qi Wang - Guangzhou Institute of Geochemistry, CAS, Guangzhou 510640, China

Kong Yang - Guangzhou Institute of Geochemistry, CAS, Guangzhou 510640, China

Hao Jiang - Guangzhou Institute of Geochemistry, CAS, Guangzhou 510640, China

Qian Cheng - Guangzhou Institute of Geochemistry, CAS, Guangzhou 510640, China

Ping Liu - Guangzhou Institute of Geochemistry, CAS, Guangzhou 510640, China

Zirui Wang - Guangzhou Institute of Geochemistry, CAS, Guangzhou 510640, China

Yun-Feng He - Guangzhou Institute of Geochemistry, CAS, Guangzhou 510640, China

Wei-Wei Hu - Guangzhou Institute of Geochemistry, CAS, Guangzhou 510640, China

Qiao-Yun Wang - School of Chemical Engineering and Technology, Guangdong Industry Polytechnic, 510300, Guangzhou, China

Jin-Yuan Xin - Institute of Atmospheric Physics, CAS, Beijing 100029, China

Yue-Si Wang - Institute of Atmospheric Physics, CAS, Beijing 100029, China

Xin-Ming Wang - Guangzhou Institute of Geochemistry, CAS, Guangzhou 510640, China

Present address: #Quan-Fu He: Institute of Energy and Climate Research, Troposphere (IEK-8), Forschungszentrum Jülich GmbH, Jülich 52428, Germany

REFERENCES

(1) Guenther, A.; Hewitt, C. N.; Erickson, D.; Fall, R.; Geron, C.; Graedel, T.; Harley, P.; Klinger, L.; Lerdau, M.; McKay, W. A.; Pierce, T.; Scholes, B.; Steinbrecher, R.; Tallamraju, R.; Taylor, J.; Zimmerman, P. A global-model of natural volatile organic-compound emissions. *J. Geophys. Res.-Atmos.* **1995,** *100*, (D5), 8873-8892.

(2) Lamarque, J. F.; Bond, T. C.; Eyring, V.; Granier, C.; Heil, A.; Klimont, Z.; Lee, D.; Liousse, C.; Mieville, A.; Owen, B.; Schultz, M. G.; Shindell, D.; Smith, S. J.; Stehfest,

E.; Van Aardenne, J.; Cooper, O. R.; Kainuma, M.; Mahowald, N.; McConnell, J. R.; Naik, V.; Riahi, K.; van Vuuren, D. P. Historical (1850-2000) gridded anthropogenic and biomass burning emissions of reactive gases and aerosols: methodology and application. *Atmos. Chem. Phys.* **2010,** *10*, (15), 7017-7039.

(3) Messina, P.; Lathiere, J.; Sindelarova, K.; Vuichard, N.; Granier, C.; Ghattas, J.; Cozic, A.; Hauglustaine, D. A. Global biogenic volatile organic compound emissions in the ORCHIDEE and MEGAN models and sensitivity to key parameters. *Atmos. Chem. Phys.* **2016,** *16*, (22), 14169-14202.

(4) Heald, C. L.; Henze, D. K.; Horowitz, L. W.; Feddema, J.; Lamarque, J.-F.; Guenther, A.; Hess, P. G.; Vitt, F.; Seinfeld, J. H.; Goldstein, A. H.; Fung, I. Predicted change in global secondary organic aerosol concentrations in response to future climate, emissions, and land use change. *J. Geophys. Res.-Atmos.* **2008,** *113*, (D5), D05211, 1-16.

(5) Hodzic, A.; Kasibhatla, P. S.; Jo, D. S.; Cappa, C. D.; Jimenez, J. L.; Madronich, S.; Park, R. J. Rethinking the global secondary organic aerosol (SOA) budget: Stronger production, faster removal, shorter lifetime. *Atmos. Chem. Phys.* **2016,** *16*, (12), 7917-7941.

(6) Bates, K. H.; Jacob, D. J. A new model mechanism for atmospheric oxidation of isoprene: Global effects on oxidants, nitrogen oxides, organic products, and secondary organic aerosol. *Atmos. Chem. Phys.* **2019,** *19*, (14), 9613-9640.

(7) Wang, Y.; Hu, M.; Guo, S.; Wang, Y.; Zheng, J.; Yang, Y.; Zhu, W.; Tang, R.; Li, X.; Liu, Y.; Le Breton, M.; Du, Z.; Shang, D.; Wu, Y.; Wu, Z.; Song, Y.; Lou, S.; Hallquist, M.; Yu, J. The secondary formation of organosulfates under interactions between biogenic emissions and anthropogenic pollutants in summer in Beijing. *Atmos. Chem. Phys.* **2018,** *18*, (14), 10693-10713.

(8) Shrivastava, M.; Andreae, M. O.; Artaxo, P.; Barbosa, H. M. J.; Berg, L. K.; Brito, J.; Ching, J.; Easter, R. C.; Fan, J. W.; Fast, J. D.; Feng, Z.; Fuentes, J. D.; Glasius, M.; Goldstein, A. H.; Alves, E. G.; Gomes, H.; Gu, D.; Guenther, A.; Jathar, S. H.; Kim, S.; Liu, Y.; Lou, S. J.; Martin, S. T.; McNeill, V. F.; Medeiros, A.; de Sa, S. S.; Shilling, J. E.; Springston, S. R.; Souza, R. A. F.; Thornton, J. A.; Isaacman-VanWertz, G.; Yee, L. D.; Ynoue, R.; Zaveri, R. A.; Zelenyuk, A.; Zhao, C. Urban pollution greatly enhances formation of natural aerosols over the Amazon rainforest. *Nat. Commun.* **2019**, *10*: 1046, 1-12.

(9) Rattanavaraha, W.; Chu, K.; Budisulistiorini, S. H.; Riva, M.; Lin, Y. H.; Edgerton, E. S.; Baumann, K.; Shaw, S. L.; Guo, H.; King, L.; Weber, R. J.; Neff, M. E.; Stone, E. A.; Offenberg, J. H.; Zhang, Z.; Gold, A.; Surratt, J. D. Assessing the impact of anthropogenic pollution on isoprene-derived secondary organic aerosol formation in PM2.5 collected from the Birmingham, Alabama, ground site during the 2013 Southern Oxidant and Aerosol Study. *Atmos. Chem. Phys.* **2016,** *16*, (8), 4897-4914.

(10) Xu, L.; Middlebrook, A. M.; Liao, J.; Gouw, J. A.; Guo, H.; Weber, R. J.; Nenes, A.; Lopez-Hilfiker, F. D.; Lee, B. H.; Thornton, J. A.; Brock, C. A.; Neuman, J. A.;

542 Nowak, J. B.; Pollack, I. B.; Welti, A.; Graus, M.; Warneke, C.; Ng, N. L. Enhanced
543 formation of isoprene-derived organic aerosol in sulfur-rich power plant plumes during
544 Southeast Nexus. *J. Geophys. Res.-Atmos.* **2016,** *121*, (18), 11,137-11,153.

545 (11) Riva, M.; Chen, Y. Z.; Zhang, Y.; Lei, Z. Y.; Olson, N. E.; Boyer, H. C.; Narayan,
546 S.; Yee, L. D.; Green, H. S.; Cui, T. Q.; Zhang, Z. F.; Baumann, K.; Fort, M.; Edgerton,
547 E.; Budisulistiorini, S. H.; Rose, C. A.; Ribeiro, I. O.; Oliveira, R. L. E.; dos Santos, E.
548 O.; Machado, C. M. D.; Szopa, S.; Zhao, Y.; Alves, E. G.; de Sa, S. S.; Hu, W. W.;
549 Knipping, E. M.; Shaw, S. L.; Duvoisin, S.; de Souza, R. A. F.; Palm, B. B.; Jimenez, J.
550 L.; Glasius, M.; Goldstein, A. H.; Pye, H. O. T.; Gold, A.; Turpin, B. J.; Vizuete, W.;
551 Martin, S. T.; Thornton, J. A.; Dutcher, C. S.; Ault, A. P.; Surratt, J. D. Increasing
552 isoprene epoxydiol-to-inorganic sulfate aerosol ratio results in extensive conversion of
553 inorganic sulfate to organosulfur forms: Implications for aerosol physicochemical
554 properties. *Environ. Sci. Technol.* **2019**, *53*, (15), 8682-8694.

555 (12) Carlton, A. G.; Pye, H. O. T.; Baker, K. R.; Hennigan, C. J. Additional benefits of
556 Federal Air-Quality Rules: Model estimates of controllable biogenic secondary organic
557 aerosol. *Environ. Sci. Technol.* **2018,** *52*, (16), 9254-9265.

558 (13) Carlton, A. G.; Wiedinmyer, C.; Kroll, J. H. A review of secondary organic aerosol
559 (SOA) formation from isoprene. *Atmos. Chem. Phys.* **2009**, *9*, (14), 4987-5005.

560 (14) Zhang, Y.; Chen, Y. Z.; Lei, Z. Y.; Olson, N. E.; Riva, M.; Koss, A. R.; Zhang, Z.
561 F.; Gold, A.; Jayne, J. T.; Worsnop, D. R.; Onasch, T. B.; Kroll, J. H.; Turpin, B. J.; Ault,
562 A. P.; Surratt, J. D. Joint impacts of acidity and viscosity on the formation of secondary

563 organic aerosol from isoprene epoxydiols (IEPDX) in phase separated particles. *Acs*
564 *Earth Space Chem.* **2019,** *3*, (22), 2646-2658.

565 (15) Paulot, F.; Wennberg, P. O. Unexpected epoxide formation in the gas-phase
566 photooxidation of isoprene. *Science* **2009,** *325*, (5941), 730-733.

567 (16) Nguyen, T. B.; Bates, K. H.; Crounse, J. D.; Schwantes, R. H.; Zhang, X.;
568 Kjaergaard, H. G.; Surratt, J. D.; Lin, P.; Laskin, A.; Seinfeld, J. H.; Wennberg, P. O.
569 Mechanism of the hydroxyl radical oxidation of methacryloyl peroxynitrate (MPAN)
570 and its pathway toward secondary organic aerosol formation in the atmosphere. *Phys.*
571 *Chem. Chem. Phys.* **2015,** *17*, (27), 17914-17926.

572 (17) McNeill, V. F. Aqueous organic chemistry in the atmosphere: Sources and chemical
573 processing of organic aerosols. *Environ. Sci. Technol.* **2015,** *49*, (3), 1237-1244.

574 (18) Eddingsaas, N. C.; VanderVelde, D. G.; Wennberg, P. O. Kinetics and products of
575 the acid-catalyzed ring-opening of atmospherically relevant butyl epoxy alcohols. *J.*
576 *Phys. Chem. A* **2010,** *114*, (31), 8106-8113.

577 (19) Surratt, J. D.; Chan, A. W.; Eddingsaas, N. C.; Chan, M.; Loza, C. L.; Kwan, A. J.;
578 Hersey, S. P.; Flagan, R. C.; Wennberg, P. O.; Seinfeld, J. H. Reactive intermediates
579 revealed in secondary organic aerosol formation from isoprene. *Proc. Natl. Acad. Sci.*
580 *U. S. A.* **2010,** *107*, (15), 6640-6645.

581 (20) Lin, Y.-H.; Zhang, H.; Pye, H. O. T.; Zhang, Z.; Marth, W. J.; Park, S.; Arashiro,
582 M.; Cui, T.; Budisulistiorini, S. H.; Sexton, K. G.; Vizuete, W.; Xie, Y.; Luecken, D. J.;

583 Piletic, I. R.; Edney, E. O.; Bartolotti, L. J.; Gold, A.; Surratt, J. D. Epoxide as a
584 precursor to secondary organic aerosol formation from isoprene photooxidation in the
585 presence of nitrogen oxides. *Proc. Natl. Acad. Sci. U. S. A.* **2013,** *110*, (17), 6718-6723.

586 (21) He, Q. F.; Ding, X.; Fu, X. X.; Zhang, Y. Q.; Wang, J. Q.; Liu, Y. X.; Tang, M. J.;
587 Wang, X. M.; Rudich, Y. Secondary organic aerosol formation from isoprene epoxides
588 in the Pearl River Delta, south China: IEPOX- and HMML-Derived Tracers. *J. Geophys.*
589 *Res.-Atmos.* **2018,** *123*, (13), 6999-7012.

590 (22) Lin, Y.-H.; Zhang, Z.; Docherty, K. S.; Zhang, H.; Budisulistiorini, S. H.;
591 Rubitschun, C. L.; Shaw, S. L.; Knipping, E. M.; Edgerton, E. S.; Kleindienst, T. E.;
592 Gold, A.; Surratt, J. D. Isoprene epoxydiols as precursors to secondary organic aerosol
593 formation: Acid-catalyzed reactive uptake studies with authentic compounds. *Environ.*
594 *Sci. Technol.* **2012,** *46*, (1), 250-258.

595 (23) Chan, M. N.; Surratt, J. D.; Claeys, M.; Edgerton, E. S.; Tanner, R. L.; Shaw, S. L.;
596 Zheng, M.; Knipping, E. M.; Eddingsaas, N. C.; Wennberg, P. O.; Seinfeld, J. H.
597 Characterization and quantification of isoprene-derived epoxydiols in ambient aerosol
598 in the Southeastern United States. *Environ. Sci. Technol.* **2010,** *44*, (12), 4590-4596.

599 (24) Lin, Y. H.; Knipping, E. M.; Edgerton, E. S.; Shaw, S. L.; Surratt, J. D.
600 Investigating the influences of SO_2 and NH_3 levels on isoprene-derived secondary
601 organic aerosol formation using conditional sampling approaches. *Atmos. Chem. Phys.*
602 **2013,** *13*, (16), 8457-8470.

603 (25) Budisulistiorini, S. H.; Li, X.; Bairai, S. T.; Renfro, J.; Liu, Y.; Liu, Y. J.; McKinney,
604 K. A.; Martin, S. T.; McNeill, V. F.; Pye, H. O. T.; Nenes, A.; Neff, M. E.; Stone, E. A.;
605 Mueller, S.; Knote, C.; Shaw, S. L.; Zhang, Z.; Gold, A.; Surratt, J. D. Examining the
606 effects of anthropogenic emissions on isoprene-derived secondary organic aerosol
607 formation during the 2013 Southern Oxidant and Aerosol Study (SOAS) at the Look
608 Rock, Tennessee ground site. *Atmos. Chem. Phys.* **2015,** *15*, (15), 8871-8888.

609 (26) Cui, T.; Zeng, Z.; dos Santos, E. O.; Zhang, Z.; Chen, Y.; Zhang, Y.; Rose, C. A.;
610 Budisulistiorini, S. H.; Collins, L. B.; Bodnar, W. M.; de Souza, R. A. F.; Martin, S. T.;
611 Machado, C. M. D.; Turpin, B. J.; Gold, A.; Ault, A. P.; Surratt, J. D. Development of a
612 hydrophilic interaction liquid chromatography (HILIC) method for the chemical
613 characterization of water-soluble isoprene epoxydiol (IEPOX)-derived secondary
614 organic aerosol. *Environ. Sci.-Proc. Imp.* **2018,** *20*, (11), 1524-1536.

615 (27) Pye, H. O. T.; Pinder, R. W.; Piletic, I. R.; Xie, Y.; Capps, S. L.; Lin, Y.-H.; Surratt,
616 J. D.; Zhang, Z.; Gold, A.; Luecken, D. J.; Hutzell, W. T.; Jaoui, M.; Offenberg, J. H.;
617 Kleindienst, T. E.; Lewandowski, M.; Edney, E. O. Epoxide pathways improve model
618 predictions of isoprene markers and reveal key role of acidity in aerosol formation.
619 *Environ. Sci. Technol.* **2013,** *47*, (19), 11056-11064.

620 (28) Riedel, T. P.; Lin, Y. H.; Zhang, Z.; Chu, K.; Thornton, J. A.; Vizuete, W.; Gold, A.;
621 Surratt, J. D. Constraining condensed-phase formation kinetics of secondary organic
622 aerosol components from isoprene epoxydiols. *Atmos. Chem. Phys.* **2016,** *16*, (3), 1245-
623 1254.

(29) Riva, M.; Bell, D. M.; Hansen, A. M. K.; Drozd, G. T.; Zhang, Z. F.; Gold, A.; Imre, D.; Surratt, J. D.; Glasius, M.; Zelenyuk, A. Effect of organic coatings, humidity and aerosol acidity on multiphase chemistry of isoprene epoxydiols. *Environ. Sci. Technol.* **2016,** *50*, (11), 5580-5588.

(30) Nestorowicz, K.; Jaoui, M.; Rudzinski, K. J.; Lewandowski, M.; Kleindienst, T. E.; Spólnik, G.; Danikiewicz, W.; Szmigielski, R. Chemical composition of isoprene SOA under acidic and non-acidic conditions: effect of relative humidity. *Atmos. Chem. Phys.* **2018,** *18*, (24), 18101-18121.

(31) Qin, M. M.; Wang, X. S.; Hu, Y. T.; Ding, X.; Song, Y.; Li, M. M.; Vasilakos, P.; Nenes, A.; Russell, A. G. Simulating biogenic secondary organic aerosol during summertime in China. *J. Geophys. Res.-Atmos.* **2018**, 123, (19), 11100-11119.

(32) Bruggemann, M.; Xu, R. S.; Tilgner, A.; Kwong, K. C.; Mutzel, A.; Poon, H. Y.; Otto, T.; Schaefer, T.; Poulain, L.; Chan, M. N.; Herrmann, H. Organosulfates in ambient aerosol: State of knowledge and future research directions on formation, abundance, fate, and importance. *Environ. Sci. Technol.* **2020,** *54*, (7), 3767-3782.

(33) Xin, J.; Wang, Y.; Pan, Y.; Ji, D.; Liu, Z.; Wen, T.; Wang, Y.; Li, X.; Sun, Y.; Sun, J. The Campaign on Atmospheric Aerosol Research Network of China: CARE-China. *B. Am. Meteorol. Soc.* **2015,** *96*, (7), 1137-1155.

(34) He, Q. F.; Ding, X.; Wang, X. M.; Yu, J. Z.; Fu, X. X.; Liu, T. Y.; Zhang, Z.; Xue, J.; Chen, D. H.; Zhong, L. J.; Donahue, N. M. Organosulfates from pinene and isoprene

644 over the Pearl River Delta, south China: Seasonal variation and implication in formation
645 mechanisms. *Environ. Sci. Technol.* **2014,** *48*, (16), 9236-9245.

646 (35) Ding, X. A.; Wang, X. M.; Zheng, M. The influence of temperature and aerosol
647 acidity on biogenic secondary organic aerosol tracers: Observations at a rural site in the
648 central Pearl River Delta region, South China. *Atmos. Environ.* **2011,** 45, (6), 1303-
649 1311.

650 (36) Piletic, I. R.; Edney, E. O.; Bartolotti, L. J. A computational study of acid catalyzed
651 aerosol reactions of atmospherically relevant epoxides. *Phys. Chem. Chem. Phys.* **2013,**
652 *15*, (41), 18065-18076.

653 (37) Gaston, C. J.; Riedel, T. P.; Zhang, Z.; Gold, A.; Surratt, J. D.; Thornton, J. A.
654 Reactive uptake of an isoprene-derived epoxydiol to submicron aerosol particles.
655 *Environ. Sci. Technol.* **2014,** *48*, (19), 11178-86.

656 (38) Marais, E. A.; Jacob, D. J.; Jimenez, J. L.; Campuzano-Jost, P.; Day, D. A.; Hu, W.;
657 Krechmer, J.; Zhu, L.; Kim, P. S.; Miller, C. C.; Fisher, J. A.; Travis, K.; Yu, K.; Hanisco,
658 T. F.; Wolfe, G. M.; Arkinson, H. L.; Pye, H. O. T.; Froyd, K. D.; Liao, J.; McNeill, V.
659 F. Aqueous-phase mechanism for secondary organic aerosol formation from isoprene:
660 Application to the southeast United States and co-benefit of SO_2 emission controls.
661 *Atmos. Chem. Phys.* **2016,** *16*, (3), 1603-1618.

662 (39) Worton, D. R.; Surratt, J. D.; LaFranchi, B. W.; Chan, A. W. H.; Zhao, Y.; Weber,
663 R. J.; Park, J.-H.; Gilman, J. B.; de Gouw, J.; Park, C.; Schade, G.; Beaver, M.; Clair, J.

664 M. S.; Crounse, J.; Wennberg, P.; Wolfe, G. M.; Harrold, S.; Thornton, J. A.; Farmer, D.
665 K.; Docherty, K. S.; Cubison, M. J.; Jimenez, J.-L.; Frossard, A. A.; Russell, L. M.;
666 Kristensen, K.; Glasius, M.; Mao, J.; Ren, X.; Brune, W.; Browne, E. C.; Pusede, S. E.;
667 Cohen, R. C.; Seinfeld, J. H.; Goldstein, A. H. Observational insights into aerosol
668 formation from isoprene. *Environ. Sci. Technol.* **2013**, *47*, (20), 11403-11413.

669 (40) Brock, C. A.; Wagner, N. L.; Anderson, B. E.; Attwood, A. R.; Beyersdorf, A.;
670 Campuzano-Jost, P.; Carlton, A. G.; Day, D. A.; Diskin, G. S.; Gordon, T. D.; Jimenez,
671 J. L.; Lack, D. A.; Liao, J.; Markovic, M. Z.; Middlebrook, A. M.; Ng, N. L.; Perring,
672 A. E.; Richardson, M. S.; Schwarz, J. P.; Washenfelder, R. A.; Welti, A.; Xu, L.; Ziemba,
673 L. D.; Murphy, D. M. Aerosol optical properties in the southeastern United States in
674 summer - Part 1: Hygroscopic growth. *Atmos. Chem. Phys.* **2016,** *16*, (8), 4987-5007.

675 (41) Stone, E. A.; Nguyen, T. T.; Pradhan, B. B.; Man Dangol, P. Assessment of
676 biogenic secondary organic aerosol in the Himalayas. *Environ. Chem.* **2012**, *9*, (3), 263-
677 272.

678 (42) Guenther, A. B.; Jiang, X.; Heald, C. L.; Sakulyanontvittaya, T.; Duhl, T.; Emmons,
679 L. K.; Wang, X. The Model of Emissions of Gases and Aerosols from Nature version
680 2.1 (MEGAN2.1): An extended and updated framework for modeling biogenic
681 emissions. *Geosci. Model Dev.* **2012**, 5, (6), 1471-1492.

682 (43) Zhang, Y. Q.; Chen, D. H.; Ding, X.; Li, J.; Zhang, T.; Wang, J. Q.; Cheng, Q.;
683 Jiang, H.; Song, W.; Ou, Y. B.; Ye, P. L.; Zhang, G.; Wang, X. M. Impact of
684 anthropogenic emissions on biogenic secondary organic aerosol: observation in the

685 Pearl River Delta, southern China. *Atmos. Chem. Phys.* **2019,** *19*, (22), 14403-14415.

686 (44) Kleindienst, T. E.; Lewandowski, M.; Offenberg, J. H.; Jaoui, M.; Edney, E. O.
687 The formation of secondary organic aerosol from the isoprene plus OH reaction in the
688 absence of NO_x. *Atmos. Chem. Phys.* **2009,** *9*, (17), 6541-6558.

689 (45) Zhang, H.; Surratt, J. D.; Lin, Y. H.; Bapat, J.; Kamens, R. M. Effect of relative
690 humidity on SOA formation from isoprene/NO photooxidation: enhancement of 2-
691 methylglyceric acid and its corresponding oligoesters under dry conditions. *Atmos.*
692 *Chem. Phys.* **2011,** *11*, (13), 6411-6424.

693 (46) Ding, X.; He, Q. F.; Shen, R. Q.; Yu, Q. Q.; Zhang, Y. Q.; Xin, J. Y.; Wen, T. X.;
694 Wang, X. M. Spatial and seasonal variations of isoprene secondary organic aerosol in
695 China: Significant impact of biomass burning during winter. *Sci. Rep.* **2016,** *6*, 20411,
696 1-10.

697 (47) Benter, T.; Liesner, M.; Schindler, R. N.; Skov, H.; Hjorth, J.; Restelli, G., REMPI-
698 MS and FTIR study of NO_2 and oxirane formation in the reactions of unsaturated-
699 hydrocarbons with NO_3 radicals. *J. Phys. Chem.* **1994,** *98*, (41), 10492-10496.

700 (48) Smith, N. R.; Crescenzo, G. V.; Huang, Y.; Hettiyadura, A. P. S.; Siemens, K.; Li,
701 Y.; Faiola, C. L.; Laskin, A.; Shiraiwa, M.; Bertram, A. K.; Nizkorodov, S. A. Viscosity
702 and liquid–liquid phase separation in healthy and stressed plant SOA. *Environ. Sci.:*
703 *Atmos*. **2021**, *1*, (3), 140-153.

704 (49) Zhang, Y.; Chen, Y. Z.; Lambe, A. T.; Olson, N. E.; Lei, Z. Y.; Craig, R. L.; Zhang,

705 Z. F.; Gold, A.; Onasch, T. B.; Jayne, J. T.; Worsnop, D. R.; Gaston, C. J.; Thornton, J.
706 A.; Vizuete, W.; Ault, A. P.; Surratt, J. D. Effect of the aerosol-phase state on secondary
707 organic aerosol formation from the reactive uptake of isoprene-derived epoxydiols
708 (IEPDX). *Environ. Sci. Technol. Lett.* **2018**, *5*, (3), 167-174.

709 (50) Zhang, Y.; Tang, L.; Sun, Y.; Favez, O.; Canonaco, F.; Albinet, A.; Couvidat, F.;
710 Liu, D.; Jayne, J. T.; Wang, Z.; Croteau, P. L.; Canagaratna, M. R.; Zhou, H.-c.; Prévôt,
711 A. S. H.; Worsnop, D. R. Limited formation of isoprene epoxydiols-derived secondary
712 organic aerosol under NO_x-rich environments in Eastern China. *Geophys. Res. Lett.*
713 **2017,** *44,* (4), 2035-2043.

714 (51) LaFranchi, B. W.; Wolfe, G. M.; Thornton, J. A.; Harrold, S. A.; Browne, E. C.;
715 Min, K. E.; Wooldridge, P. J.; Gilman, J. B.; Kuster, W. C.; Goldan, P. D.; de Gouw, J.
716 A.; McKay, M.; Goldstein, A. H.; Ren, X.; Mao, J.; Cohen, R. C. Closing the peroxy
717 acetyl nitrate budget: Observations of acyl peroxy nitrates (PAN, PPN, and MPAN)
718 during BEARPEX 2007. *Atmos. Chem. Phys.* **2009**, *9*, (19), 7623-7641.

719 (52) Riva, M.; Budisulistiorini, S. H.; Zhang, Z.; Gold, A.; Surratt, J. D. Chemical
720 characterization of secondary organic aerosol constituents from isoprene ozonolysis in
721 the presence of acidic aerosol. *Atmos. Environ.* **2016**, *130*, 5-13.

722 (53) Riva, M.; Budisulistiorini, S. H.; Chen, Y. Z.; Zhang, Z. F.; D'Ambro, E. L.; Zhang,
723 X.; Gold, A.; Turpin, B. J.; Thornton, J. A.; Canagaratna, M. R.; Surratt, J. D. Chemical
724 characterization of secondary organic aerosol from oxidation of isoprene
725 hydroxyhydroperoxides. *Environ. Sci. Technol.* **2016**, *50*, (18), 9889-9899.

(54) Jaoui, M.; Piletic, I. R.; Szmigielski, R.; Rudzinski, K. J.; Lewandowski, M.; Riedel, T. P.; Kleindienst, T. E. Rapid production of highly oxidized molecules in isoprene aerosol via peroxy and alkoxy radical isomerization pathways in low and high NO_x environments: Combined laboratory, computational and field studies. *Sci. Total Environ.* **2021**, *775*, 145592, 1-10.

(55) Jaoui, M.; Szmigielski, R.; Nestorowicz, K.; Kolodziejczyk, A.; Sarang, K.; Rudzinski, K. J.; Konopka, A.; Bulska, E.; Lewandowski, M.; Kleindienst, T. E. Organic hydroxy acids as highly oxygenated molecular (HOM) tracers for aged isoprene aerosol. *Environ. Sci. Technol.* **2019**, *53*, (24), 14516-14527.

(56) Lopez-Hilfiker, F. D.; Mohr, C.; D'Ambro, E. L.; Lutz, A.; Riedel, T. P.; Gaston, C. J.; Iyer, S.; Zhang, Z.; Gold, A.; Surratt, J. D.; Lee, B. H.; Kurten, T.; Hu, W. W.; Jimenez, J.; Hallquist, M.; Thornton, J. A. Molecular composition and volatility of organic aerosol in the southeastern U.S.: Implications for IEPOX derived SOA. *Environ. Sci. Technol.* **2016**, *50*, (5), 2200-2209.

(57) Cope, J. D.; Abellar, K. A.; Bates, K. H.; Fu, X.; Nguyen, T. B. Aqueous photochemistry of 2-Methyltetrol and erythritol as sources of formic acid and acetic acid in the atmosphere. *Acs Earth Space Chem.* **2021**, *5*, (6), 1265-1277.

(58) Chen, Y.; Zhang, Y.; Lambe, A. T.; Xu, R.; Lei, Z.; Olson, N. E.; Zhang, Z.; Szalkowski, T.; Cui, T.; Vizuete, W.; Gold, A.; Turpin, B. J.; Ault, A. P.; Chan, M. N.; Surratt, J. D. Heterogeneous hydroxyl radical oxidation of isoprene epoxydiol-derived methyltetrol sulfates: Plausible formation mechanisms of previously unexplained

747 organosulfates in ambient fine aerosols. *Environ. Sci. Technol. Lett.* **2020,** *7*, (7), 460-
748 468.

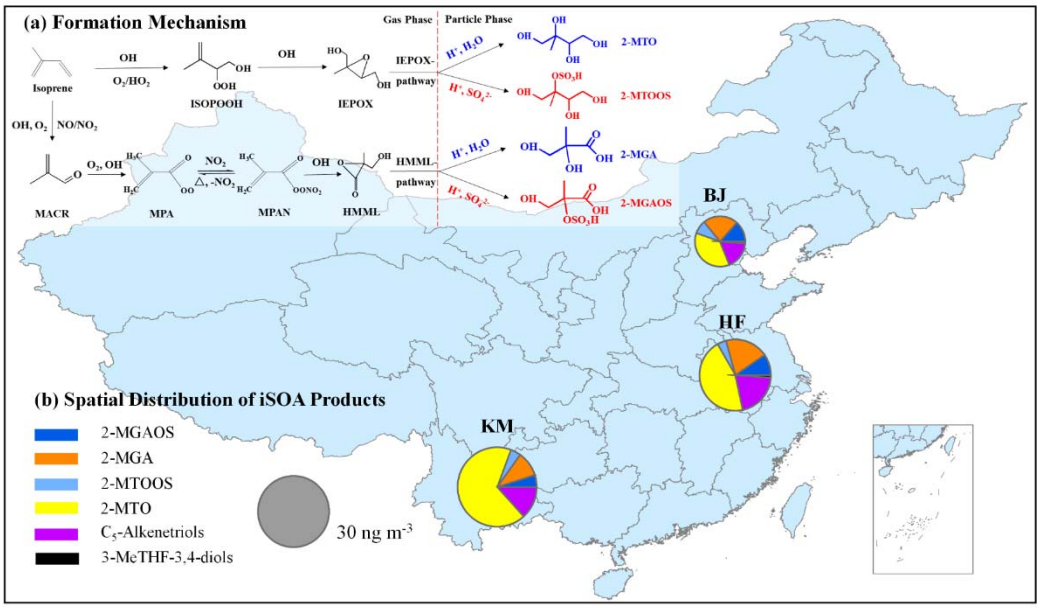

749

750 **Figure 1** Formation processes of iOTs (compounds marked in blue) and iOSs
751 (compounds marked in red) through epoxides pathway (a); Chemical composition and
752 spatial distribution of iSOA products (b); KM has the highest concentrations of iSOA
753 products and 2-MTO is the major species among these iSOA products. In (b), gray circle
754 indicates total concentration of iSOA products on an annual average basis and the size
755 of the circle reflects the scale of concentrations.

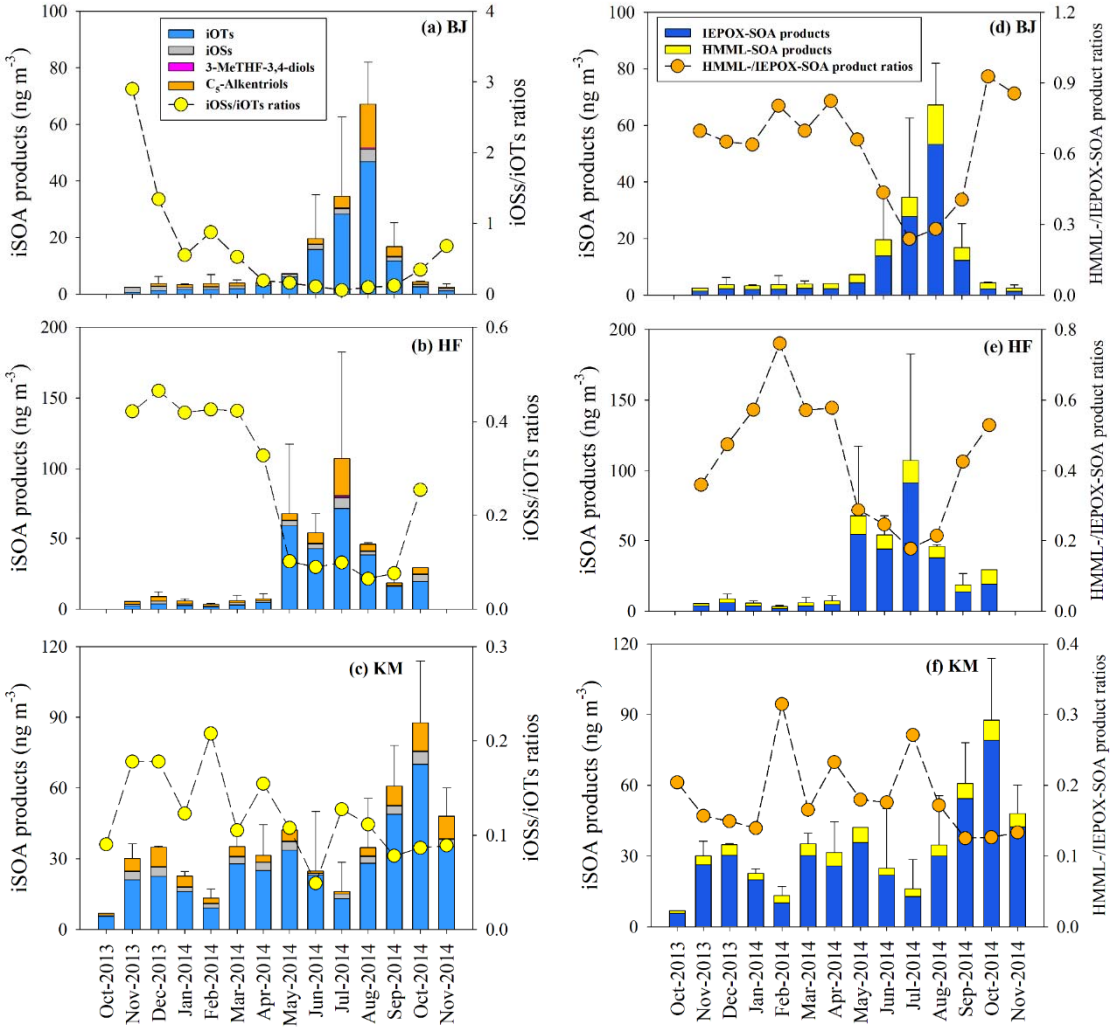

Figure 2 Monthly variations of iSOA products (a-f), iOSs/iOTs ratios (a-c) and HMML-/IEPOX-SOA products ratios (d-f) at three sites. iSOA products concentrations are high in summer and low in winter. Ratios of iOSs to iOTs and ratios of HMML-/IEPOX-SOA products are high in winter and low in summer.

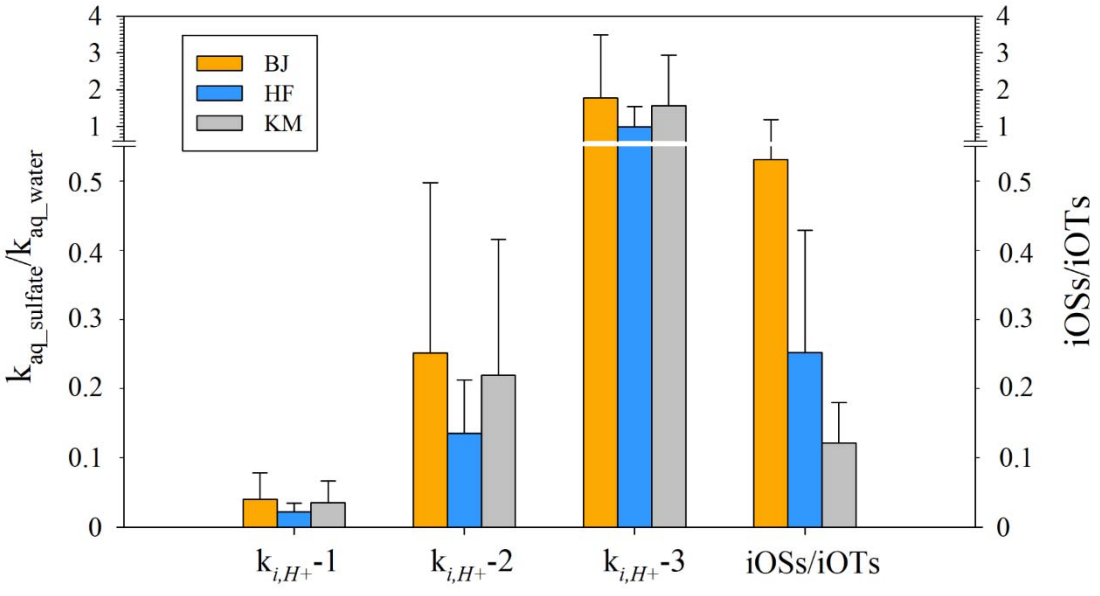

761

762 **Figure 3** Comparison between iOSs/iOTs observed at three sites and $k_{aq\_sulfate}/k_{aq\_water}$

763 calculated using different set of $k_{i,j}$ values ($k_{i,H+}$-1, $k_{i,H+}$-2 and $k_{i,H+}$-3 were suggested

764 by Pye et al., 2013, Riedel et al., 2016 and Piletic et al., 2013, respectively).[27, 28, 36]

765 There is an apparent disagreement in spatial gradience between observation and models.

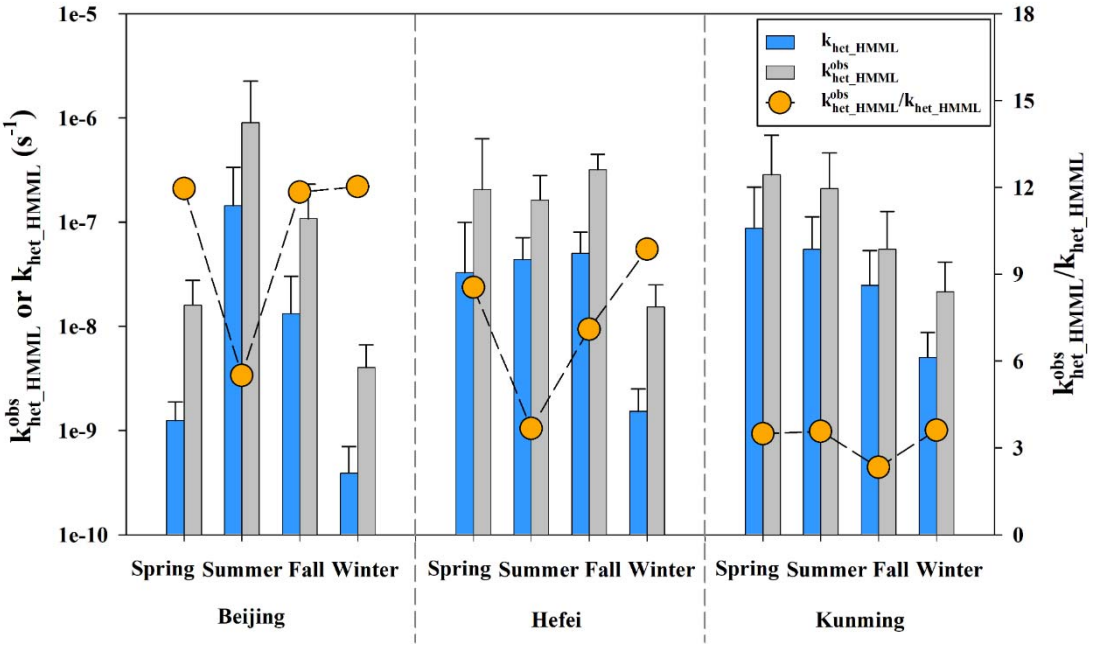

766

767 **Figure 4** Comparison of $k^{obs}_{het\_HMML}$ and k_{het_HMML} in different seasons at three sites.

768 Observation-constrained $k^{obs}_{het\_HMML}$ values are 3-10 times higher than k_{het_HMML} values

769 estimated using the kinetic parameters of IEPOX provided by $k_{i,H+}$-1 (Pye et al.,

770 2013).[27]